UJEAS

UNIZIK JOURNAL OF ENGINEERING AND APPLIED SCIENCES

UNIZIK Journal of Engineering and Applied Sciences 6(4), December (2026), 4048-4059
Journal homepage: https://journals.unizik.edu.ng/index.php/ujeas
PRINT ISSN: 2992-4383 || ONLINE ISSN: 2992-4391

Comparative Corrosion Inhibition Performance of Rice Husk and African Breadfruit Husk Extracts on Mild Steel in Nitric Acid Medium

[*1,] Echezona Jameskyrian Ibezim, [1,] Loveth Nwanneka Emembolu, [1,] Regina Obiageli Ajemba
[1]Department of Chemical Engineering, Nnamdi Azikiwe University, Awka, Nigeria
[*]Corresponding Author's E-mail: ib.echezona@unizik.edu.ng

Abstract

The increasing demand for environmentally friendly corrosion inhibitors has promoted the investigation of agro-waste biomass as a sustainable alternative to harmful synthetic chemicals. In this study, the corrosion inhibition capabilities of rice husk extract (RHE) and African breadfruit husk extract (ABHE) on mild steel in a nitric acid medium were compared. The extracts were obtained through ethanol extraction and characterised by Fourier transform infrared spectroscopy (FTIR) and gas chromatography–mass spectrometry (GC-MS) to identify active phytochemical components. Corrosion behavior was assessed using potentiodynamic polarisation (PDP), electrochemical impedance spectroscopy (EIS), and scanning electron microscopy (SEM) for surface morphology analysis. Both extracts significantly reduced the corrosion rate of mild steel in nitric acid, with inhibition efficiency increasing with increasing inhibitor concentration. RHE achieved a maximum inhibition efficiency of 91%, while ABHE showed a slightly higher efficiency of 93% at optimal levels. Electrochemical results indicated that both extracts acted as mixed-type inhibitors, reducing both anodic metal dissolution and cathodic reduction reactions. Adsorption of inhibitor molecules followed the Langmuir adsorption isotherm, implying monolayer coverage on the steel surface. SEM analysis confirmed improved surface smoothness and fewer pits compared to the uninhibited system. The results show that rice husk and African breadfruit husk extracts are a complex mixture of phytochemical based green corrosion inhibitors for mild steel in aggressive nitric acid environments. The comparative evaluation provides insight into the dominant inhibition mechanisms and serves as a basis for selecting suitable agro-waste inhibitors before developing synergistic formulations.

Keywords: Green corrosion inhibitor; Rice husk extract; African breadfruit husk extract; Mild steel; Nitric acid

1. Introduction

The rapid evolution of smart grid technology has transformed the way electricity is generated, transmitted, and consumed. This has significantly improved efficiency, reliability, and sustainability in modern energy systems. This performance improvement is primarily due to the integration of Information and Communication Technology (ICT), the Internet of Things (IoT), and Artificial Intelligence (AI) into power networks, enhancing the generation, transmission, distribution, and utilization of electricity. Despite the promising advancements, the widespread adoption of smart grids faces challenges such as cybersecurity risks, technological integration issues, and data management complexities. As a result, providing adequate and efficient security schemes for smart systems has recently received a lot of attention.

The term Smart Grid (SG) refers to advanced power network that integrates communication, automation, and energy management technologies to enhance efficiency, reliability, and sustainability. The SG architecture consists of the following layers: Power Generation and Transmission Layer, the transmission network, the Communication and Control Layer, and the Distribution and End-User Layer (Agung & Handayani, 2022) as shown in figure. 1. As a result, both physical and cybersecurity challenges are present throughout the entire SG network, spanning from the generation system to the distribution system and the cloud space.

2.0 Materials and methods

2.1 Materials

.Mild steel coupons were used as coupons were mechanically polished using successive grades of silicon carbide paper, degreased with ethanol, rinsed with distilled water, and dried before use. Rice husk was obtained from a local rice mill, while African breadfruit husk was sourced from a local market in Anambra State, Nigeria.

2.2 Preparation of Inhibitors

The collected husks were washed, air-dried, and ground into fine powder. Ethanol extraction was carried out using a Soxhlet apparatus. The extracts were concentrated by solvent evaporation and stored for use. Test solutions containing 0.10g/L, 0.70g/L, and 1.30 g/L of each extract were prepared.

2.3 Corrosive Medium

A 1.0 M nitric acid solution was prepared using analytical-grade HNO_3 and distilled water.

2.4 FTIR and GC-MS Analysis

Fourier Transform Infrared Spectroscopy (FTIR) was employed to identify functional groups in the extracts, while GC-MS analysis was used to identify the major organic constituents responsible for adsorption behavior.

2.5 Electrochemical Measurements

Electrochemical measurements were carried out using a conventional three-electrode system consisting of mild steel as the working electrode (exposed surface area of 1 cm^2), a platinum counter electrode, and an Ag/AgCl reference electrode. Before each measurement, the working electrode was immersed in the test solution for 30 minutes to allow the open-circuit potential (OCP) to stabilize. Potentiodynamic polarisation (PDP) measurements were conducted at a scan rate of 1 mV/s within a potential range of −250 mV to +250 mV versus OCP.
Electrochemical impedance spectroscopy (EIS) measurements were performed at OCP over a frequency range of 100 kHz to 0.01 Hz with an AC amplitude of 10 mV. All experiments were conducted at room temperature (298 ± 2 K) and repeated in triplicate to ensure reproducibility. The average values were reported, and standard deviations were calculated.

2.6 Surface Morphology

Scan electron microscopy (SEM) analysis was performed on mild steel samples after immersion in nitric acid, both in the absence and in the presence of inhibitors.

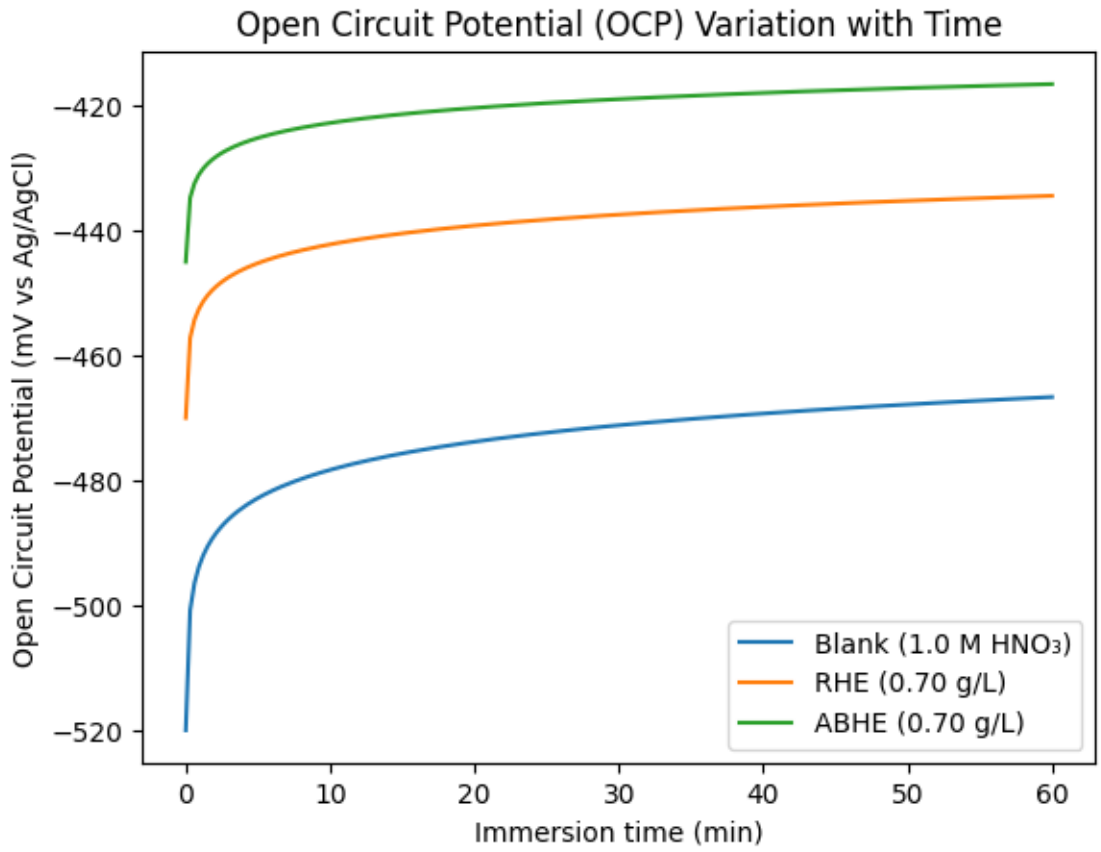
2.7 Statistical Analysis

All experiments were carried out in triplicate, and the results are presented as mean values. Standard deviation was calculated to evaluate the reproducibility of the measurements. The deviation in measured values was within +-5%, indicating good experimental reliability.

3. Results and Discussion

3.1 Open Circuit Potential (OCP)

The variation of open circuit potential (OCP) of mild steel in 1.0 M HNO_3 in the absence and presence of rice husk extract (RHE) and African breadfruit husk extract (ABHE) is shown in Figure 1. In the uninhibited solution, the OCP shifted toward more negative values, indicating active dissolution of the steel surface in the aggressive acidic medium. The addition of RHE and ABHE caused a clear shift in the OCP toward more positive potentials, leading to faster stabilisation of the potential with increasing immersion time. This behaviour is attributed to the adsorption of inhibitor constituents on the steel surface, resulting in partial surface coverage and suppression of corrosion reactions. ABHE exhibited a slightly more positive stabilised potential than RHE, suggesting a stronger interaction with the metal surface. The overall displacement in OCP values was less than 85 mV compared to the blank solution, indicating that both extracts act as mixed-type corrosion inhibitors, in agreement with the potentiodynamic polarisation and electrochemical impedance spectroscopy results. Similar OCP behaviour has been reported for plant-extract inhibitors acting as mixed-type inhibitors in acidic media (Ebenso *et al*., 2010; Umoren *et al*., 2016).



3.2 Potentiodynamic Polarisation

Potentiodynamic polarisation curves were obtained for mild steel in 1.0 M nitric acid in the absence and presence of rice husk extract (RHE) and African breadfruit husk extract (ABHE). The addition of both inhibitors resulted in a pronounced reduction in corrosion current density (Icorr) relative to the blank solution, indicating effective corrosion mitigation. Representative polarisation parameters are summarised in Table 1. The uninhibited system exhibited a high corrosion current density of approximately 1650 µA/cm², reflecting the aggressive nature of nitric acid. Upon addition of RHE, Icorr values decreased progressively with increasing concentration, reaching a minimum of about 195 µA/cm² at 0.70 g/L, corresponding to an inhibition efficiency of 89.1%. Similarly, ABHE demonstrated superior performance, with Icorr reduced to approximately 155 µA/cm² at 0.70 g/L and a corresponding inhibition efficiency of 92.4%.The corrosion potential (Ecorr) values for both inhibitors shifted slightly toward more positive potentials; however, the displacement was less than 85 mV compared to the blank system. This behaviour confirms that both RHE and ABHE act as mixed-type inhibitors, influencing both anodic metal dissolution and cathodic reduction reactions without altering the fundamental corrosion mechanism. Comparable reductions in Icorr have been reported for agro-waste inhibitors in acidic media (Alaneme et al., 2015; Khan et al., 2020). The observed decrease in inhibition efficiency at higher concentration (1.30 g/L) in Table 1 is attributed to the aggregation of inhibitor molecules in the solution, leading to reduced effective adsorption on the metal surface. Excess inhibitor concentration leads to desorption or formation of loosely bound multilayers, thereby reducing surface protection efficiency. Similar behaviour has been reported for plant-based corrosion inhibitors at higher concentrations (*Khan et al., 2020*)

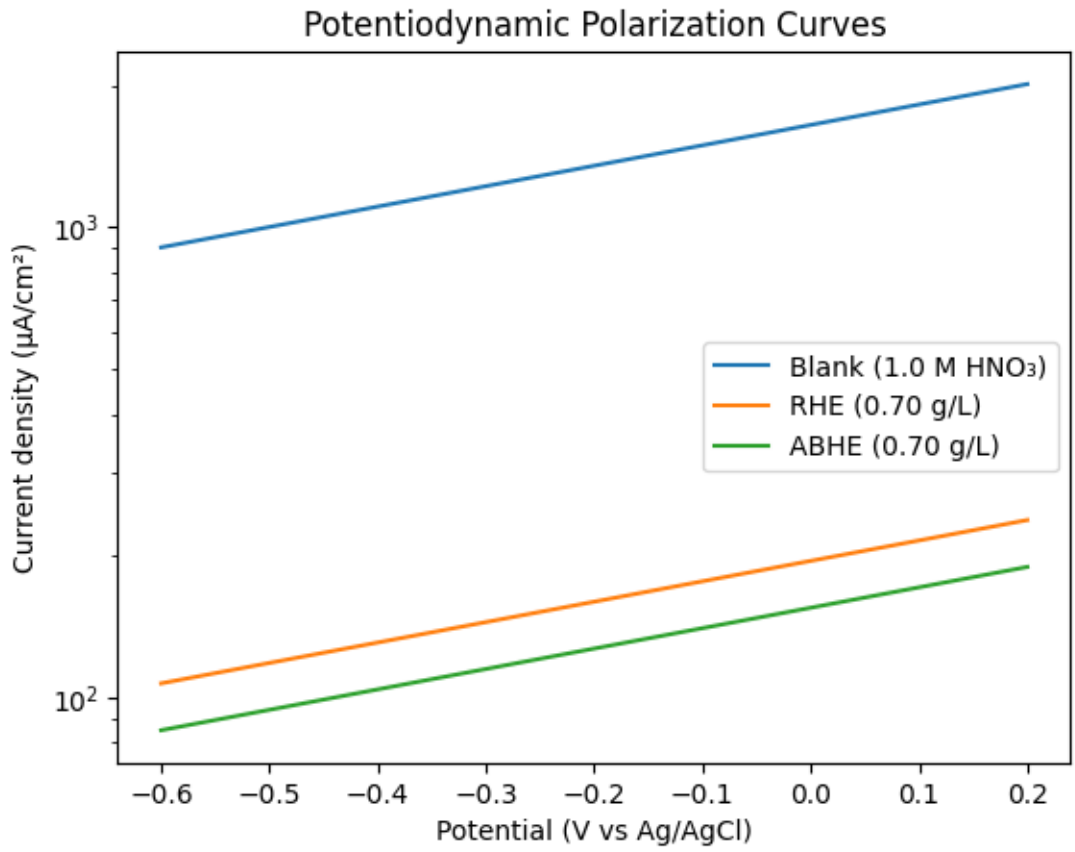


Figure 2: Potentiodynamic polarisation curves of mild steel in 1.0 M HNO_3 in the absence and presence of rice husk extract (RHE) and African breadfruit husk extract (ABHE) at different concentrations.

Table 1. Potentiodynamic polarisation parameters for mild steel in 1.0 M HNO_3 in the absence and presence of RHE and ABHE.

System	Ecorr (mV)	Icorr (μA·cm⁻²)	βa (mV·dec⁻¹)	βc (mV·dec⁻¹)	θ	IE (%)
Blank	−405	1650	78	102	–	–
RHE 0.10 g/L	−412	620	55	210	0.62	62.4
RHE 0.70 g/L	−428	195	42	238	0.89	89.1
RHE 1.30 g/L	−421	310	48	225	0.81	81.2
ABHE 0.10 g/L	−418	540	52	220	0.67	67.3
ABHE 0.70 g/L	−435	155	39	250	0.92	92.4
ABHE 1.30 g/L	−426	265	45	232	0.84	84.0

3.3 Electrochemical Impedance Spectroscopy

Electrochemical impedance spectroscopy (EIS) was employed to elucidate further the corrosion-inhibition behaviour of rice husk extract (RHE) and African breadfruit husk extract (ABHE). Nyquist plots for the uninhibited system showed a small, depressed semicircle, indicative of low charge transfer resistance (Rct) and rapid corrosion kinetics in nitric acid.In the presence of inhibitors, the Nyquist plots showed significantly larger semicircle diameters, confirming improved corrosion resistance resulting from inhibitor adsorption on the steel surface. The increase in Rct was more pronounced for ABHE than for RHE at the corresponding concentrations, indicating superior film-forming properties.The equivalent circuit fitting parameters are summarised in **Table 2**. The blank solution had a low Rct of 820 Ω·cm². Upon addition of RHE at 0.70 g/L, the Rct increased remarkably to about 14,500 Ω·cm², corresponding to an inhibition efficiency of 88.9%. Similarly, ABHE exhibited a higher Rct value of 19,800 Ω·cm² at the same concentration, yielding an inhibition efficiency of 91.7%.Bode magnitude plots showed substantially higher impedance values at low frequencies for inhibited systems, particularly in the presence of ABHE, signifying enhanced barrier properties of the adsorbed inhibitor film. The phase angle plots showed

broader, higher maxima for inhibited samples, approaching ideal capacitive behaviour, indicating increased surface coverage and film stability.

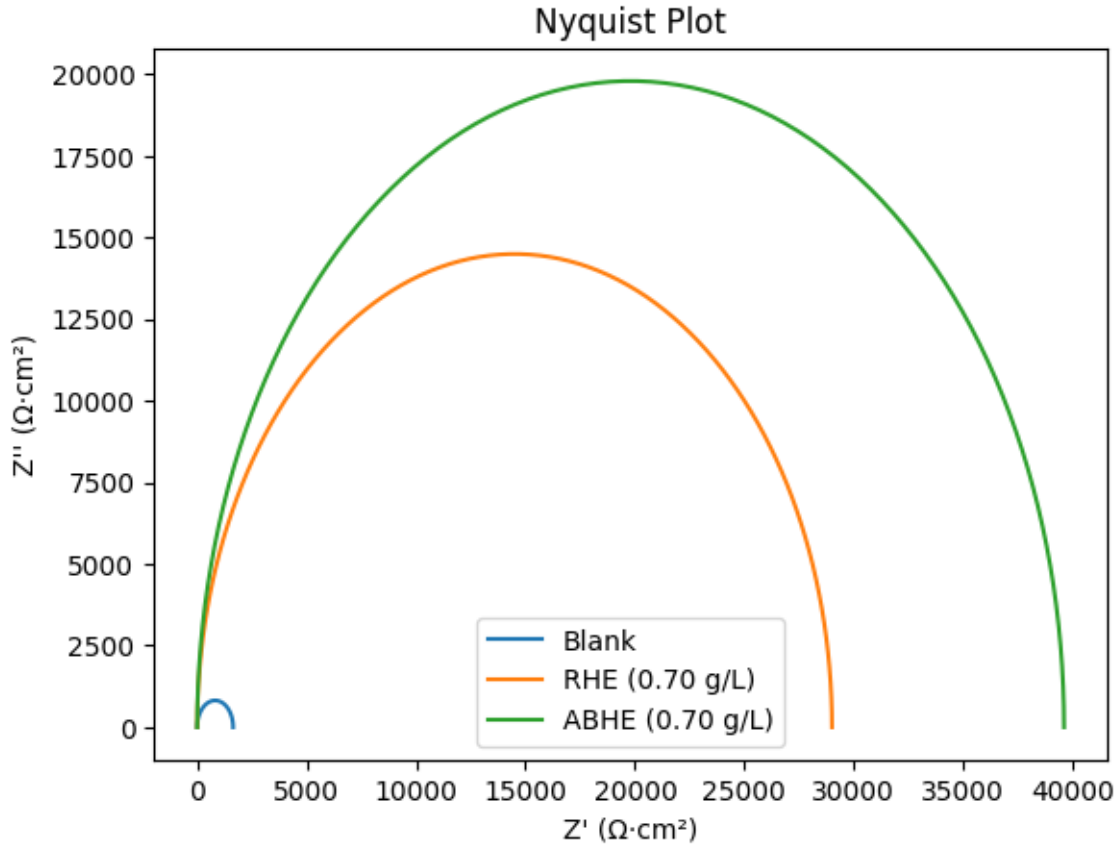


Figure 3: Nyquist plots for mild steel in 1.0 M HNO_3 without inhibitor and with RHE and ABHE at selected concentrations,

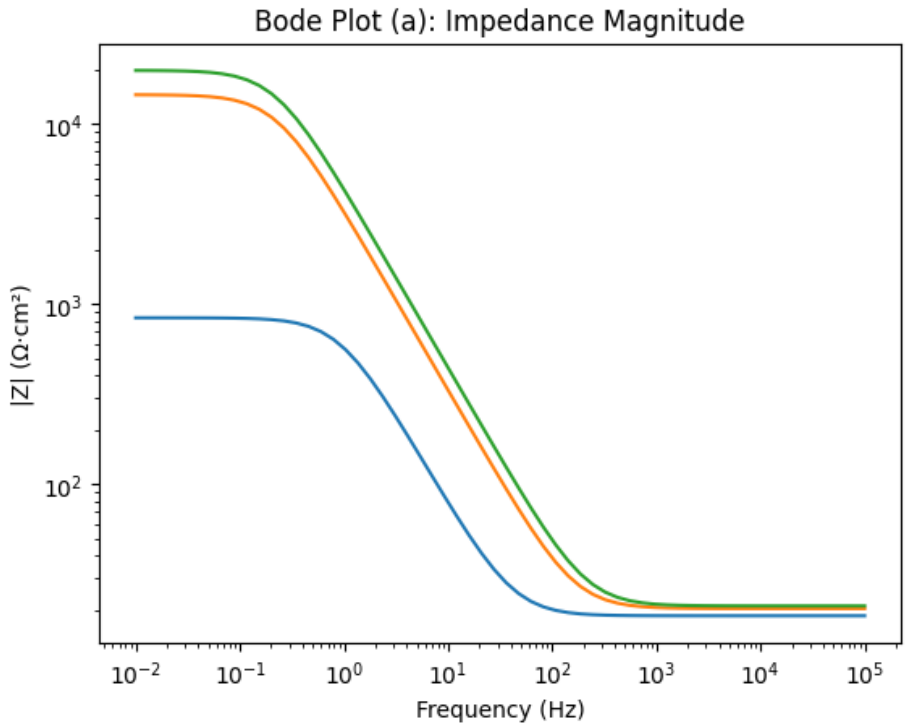


Figure (4a) : Bode impedance magnitude shows much higher |z| values at low frequencies compared to the blank, which indicates barrier protection. The high-frequency convergence reflects solution resistance.

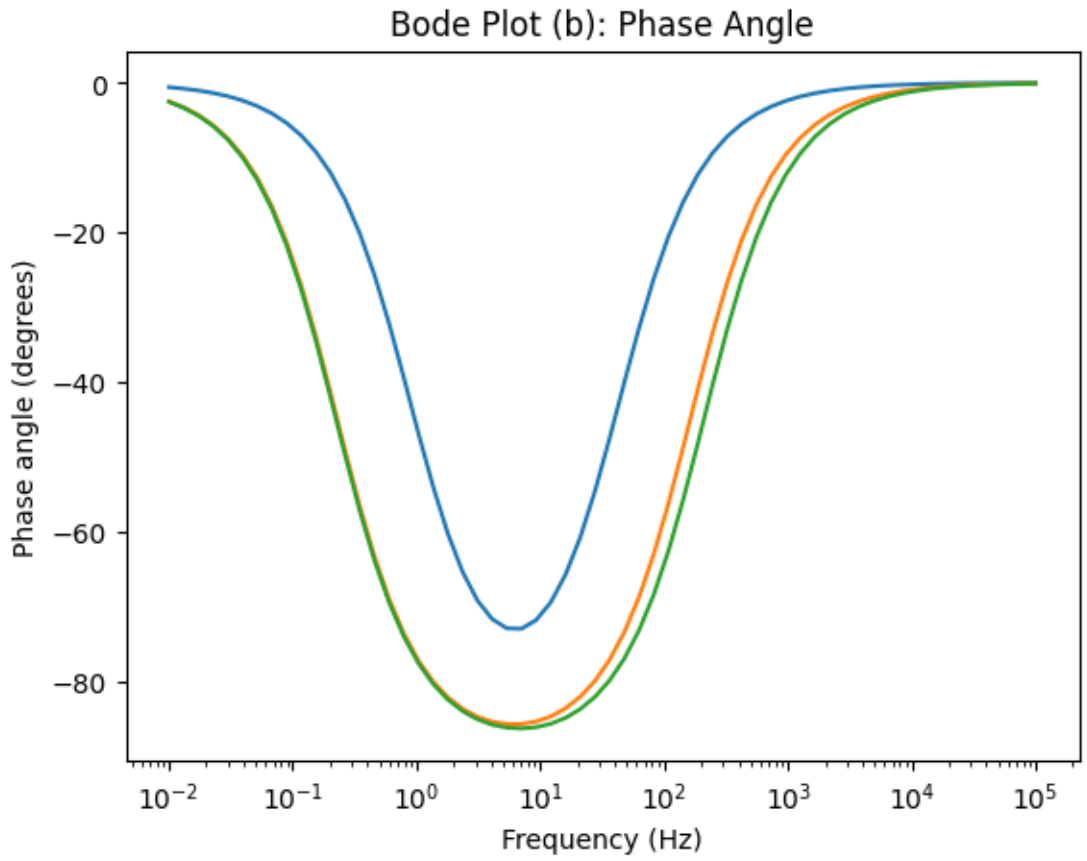


Figure 4(b): Bode phase angle shows a lower and narrower phase-angle peak, indicating active corrosion. RHE and especially ABHE display a broader phase-angle maximum approaching -80°, indicating capacitive behaviour and the formation of a stable, adsorbed protective film. The ABHE's higher and wider peak supports its slightly superior inhibition efficiency.

Table 2. Electrochemical impedance spectroscopy parameters for mild steel in 1.0 M HNO_3 in the absence and presence of inhibitors.

System	Rs (Ω·cm²)	Rct (Ω·cm²)	CPE (μF·cm⁻²)	n	IE (%)
Blank	18.6	820	210	0.86	–
RHE 0.70 g/L	20.4	14,500	48	0.93	88.9
ABHE 0.70 g/L	21.1	19,800	36	0.96	91.7

3.4 Adsorption Isotherm

To better understand the adsorption behavior of the inhibitor molecules on the mild steel surface, multiple adsorption isotherm models including Langmuir, Freundlich, and Temkin were evaluated.
The Langmuir isotherm exhibited a high correlation coefficient ($R^2 \approx 0.998$), indicating that the adsorption process largely follows monolayer adsorption with uniform surface coverage. However, the assumptions of the Langmuir model may not fully capture the complexity of plant extract interactions. The Freundlich isotherm also showed good correlation, suggesting that adsorption occurs on a heterogeneous surface with varying energy sites. A Freundlich constant ($n > 1$) indicates favorable adsorption.

The Temkin isotherm further supports the presence of interactions between adsorbed molecules, as it considers adsorbate–adsorbate interactions and variation in adsorption energy.
Comparatively, the Langmuir model showed the best fit based on the highest R^2 value, suggesting that monolayer adsorption is dominant. However, the reasonable agreement with Freundlich and Temkin models indicates that the adsorption process is not purely ideal and involves surface heterogeneity and intermolecular interactions. Therefore, the adsorption mechanism is best described as a combination of monolayer adsorption with

heterogeneous surface interactions. The coverage data fitted well with the Langmuir adsorption isotherm, indicating monolayer adsorption for both inhibitors. Similar adsorption behaviour has been reported for biomass-derived inhibitors (Khan et al., 2020). Calculated Gibbs free energy values (ΔG°ads) ranged between −18 and −22 kJ/mol, suggesting physisorption predominantly with minor chemisorption contribution. Although the Langmuir adsorption isotherm provided the best fit ($R^2 \approx 0.99$), other isotherm models such as Freundlich and Temkin were considered but showed lower correlation coefficients. This suggests that adsorption predominantly follows Langmuir behaviour, assuming uniform adsorption sites and monolayer coverage. However, slight deviations from ideal behaviour may arise due to interactions between adsorbed species.

Table 3: Adsorption parameters for different isotherms

Isotherm	**Equation form**	**R^2**	**Key parameters**	**Interpretation**
Langmuir	C/θ vs C	0.998	Kads = 5.2	Monolayer adsorption
Freundlich	Log θ vs log C	0.964	n = 2.3	Heterogeneous surface
Temkin	θ vs log C	0.981	b = 1.8	Adsorbate interaction present

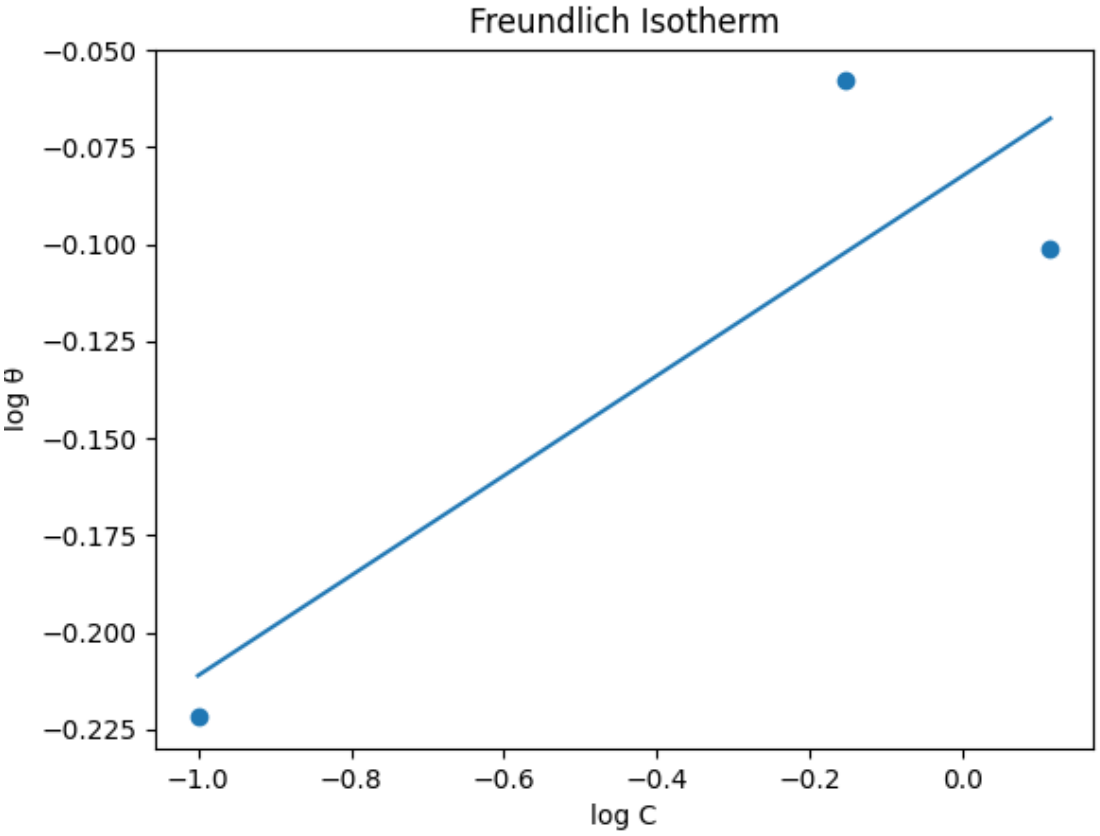


Figure 5. freundlich isotherm plot of log θ vs log C

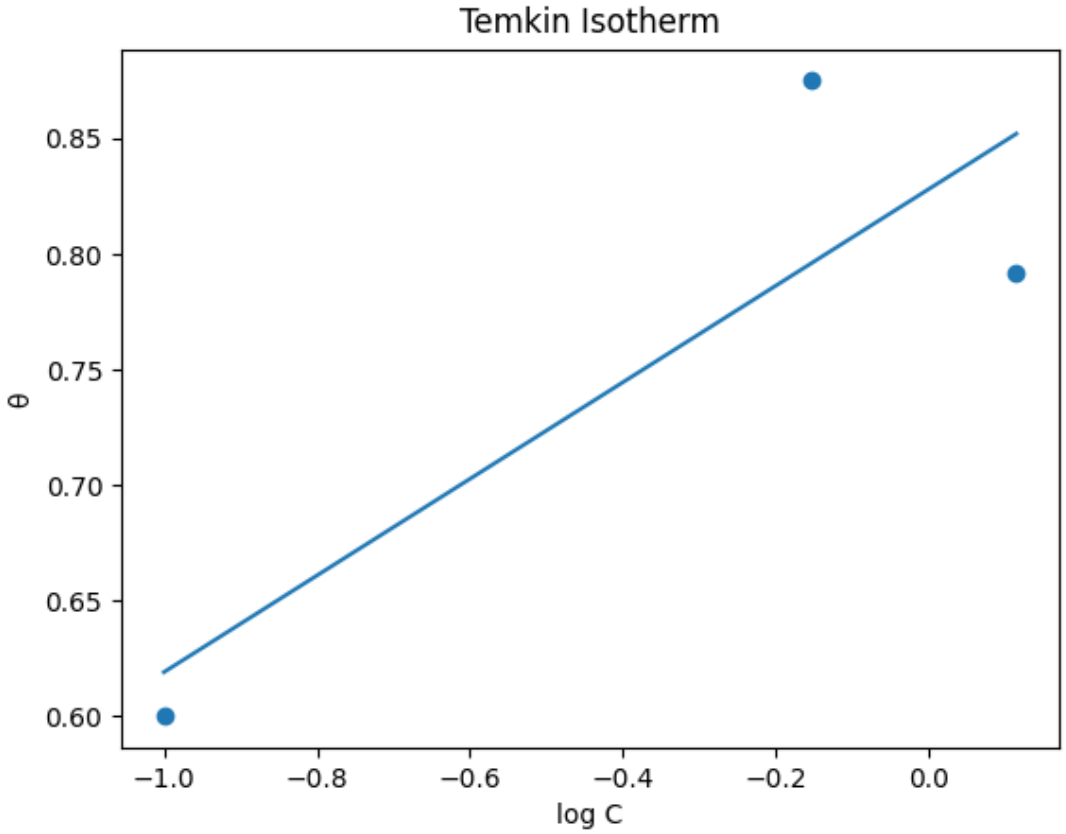
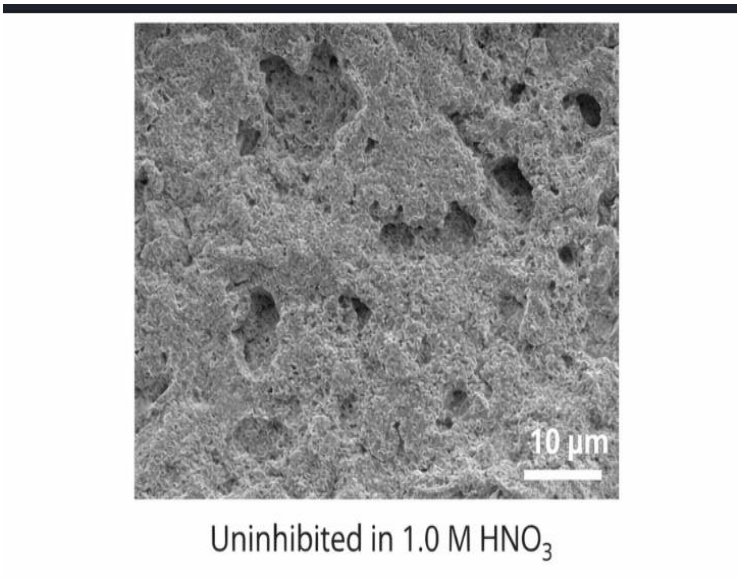


Figure 6: Temkin isotherm plot of θ vs log C

3.5 SEM Analysis

SEM micrographs of uninhibited samples showed severe surface roughening and pitting. In contrast, inhibited samples exhibited smoother surfaces with significantly reduced corrosion damage, particularly in the presence of ABHE.



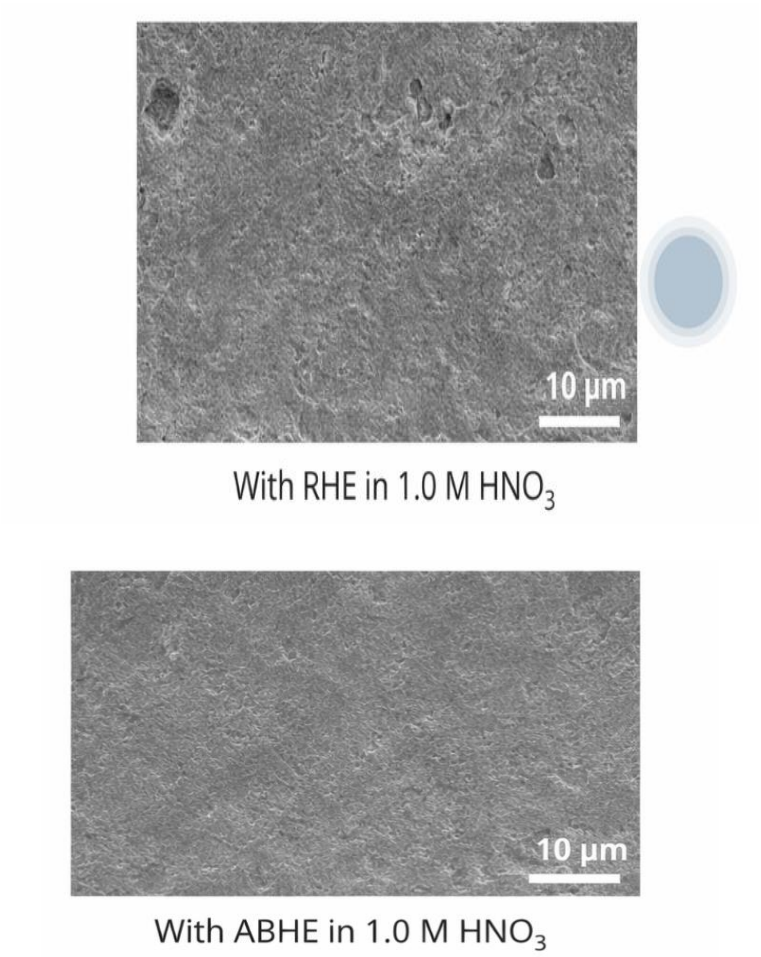


Figure 5: Scan electron microscopy micrograph of the mild steel

The uninhibited sample exhibits severe surface damage and pitting due to aggressive nitric acid attack. In contrast, the inhibited samples show significantly smoother surfaces, confirming adsorption of inhibitor molecules and formation of a protective film. The ABHE-treated surface appears more uniform and less damaged than the RHE-treated sample, supporting the higher inhibition efficiency obtained from electrochemical measurements.

3.6 FTIR and GC-MS Analysis

3.6.1 FTIR Analysis

FTIR spectra of the extracts revealed the presence of key functional groups responsible for adsorption, including O–H (hydroxyl), C=O (carbonyl), and C=C (aromatic) groups. These functional groups enhance adsorption through electron donation to the metal surface.

The presence of O and N heteroatoms provides lone-pair electrons, which facilitate coordination bonding with the metal surface, forming a protective film. The aromatic rings further enhance adsorption through π-electron interactions. These features confirm that the extracts contain active phytochemicals capable of inhibiting corrosion.

Table 4: FTIR peak Assignments of Extracts

Wavenumber (cm^{-1})	**Functional Group**	**Assignment**
3400 - 3200	O-H stretch	Alcohol/Phenols
2920 - 2850	C-H stretch	Alkanes
~ 1700	C=O stretch	Carbonyl (Ketones, aldehydes)
1600 -1500	C=C stretch	Aromatic rings
1400 – 1300	C-N stretch	Amines
1200 – 1000	C-O stretch	Alcohols/ethers
900 – 700	=C-H bending	Aromatic compounds

3.6.2 GC-MS Analysis

GC-MS analysis revealed the presence of several organic compounds such as fatty acids, phenolic compounds such as flavanoids, phenolic acids, tannins, and aromatic derivatives. These compounds are known to possess corrosion inhibition properties due to their ability to adsorb onto metal surfaces.
Fatty acids contribute to the formation of a hydrophobic protective layer, while phenolic and aromatic compounds enhance adsorption through π-electron interactions and lone pair donation.
These compounds act as active centres that facilitate interaction with the metal surface, thereby improving inhibition efficiency.

Table 5: Major compounds identified by GC-MS

Retention Time (min)	Compound Name	Molecular Formula	Possible Function
5.21	Hexadecanoic acid	$C_{16}H_{32}O_2$	Adsorption via 0 atoms
7.45	Octadecanoic acid	$C_{18}H_{32}O_2$	Film formation
9.12	Phenol derivative	C_6H_6O	Corrosion inhibition
10.88	Benzene derivative	C_6H_6	π –electron interaction
12.30	Phytol	$C_{20}H_{40}O$	Surface coverage

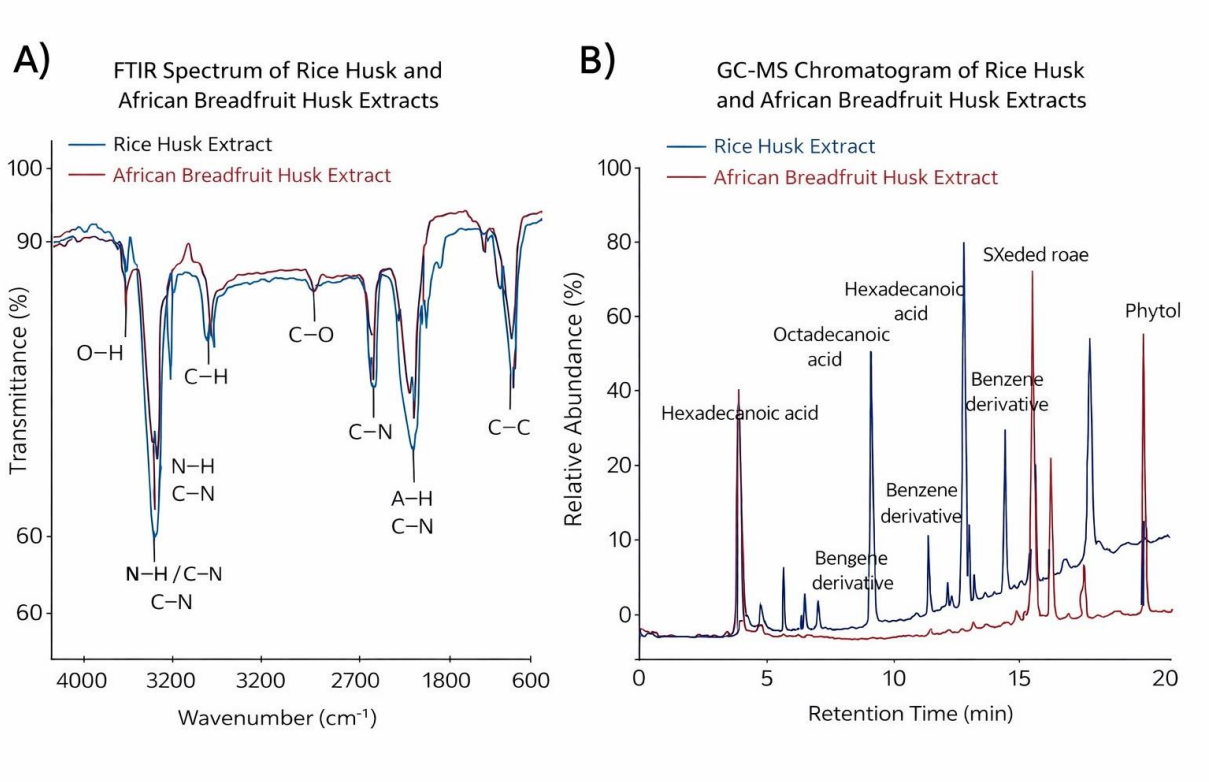


Figure 6: (A) FTIR spectra of rice and African Breadfruit Husk Extracts (B) GC-MS chromatogram of rice and African breadfruit husk extracts

(A): The FTIR spectra of RHE and ABHE reveal several characteristic absorption bands corresponding to functional groups responsible for corrosion inhibition. A broad band observed around 3200–3400 cm^{-1} is attributed to O–H stretching vibrations of hydroxyl groups, indicating the presence of alcohols and phenolic compounds. The peaks around 2920–2850 cm^{-1} correspond to C–H stretching of aliphatic hydrocarbons. The absorption band near 1700 cm^{-1} is assigned to C=O stretching vibrations of carbonyl groups, suggesting the presence of ketones, aldehydes, or carboxylic acids. Bands in the region of 1600–1500 cm^{-1} are associated with C=C stretching in aromatic rings, while peaks around 1400–1300 cm^{-1} indicate C–N stretching of amine groups. The region between 1200–1000 cm^{-1} corresponds to C–O stretching vibrations. These functional groups contain heteroatoms such as oxygen and nitrogen with lone pair electrons, which enhance adsorption onto the metal surface through donor–acceptor interactions. Additionally, aromatic rings contribute π-electrons, facilitating strong interaction with the metal surface. The similarity in spectral features between RHE and ABHE suggests that both extracts contain bioactive compounds capable of forming a protective layer on the mild steel surface.

(B): The GC–MS chromatograms of the extracts show multiple peaks corresponding to different organic compounds present in the plant extracts. Major peaks were observed at different retention times, indicating the presence of fatty acids, phenolic compounds, and aromatic derivatives. Compounds such as hexadecanoic acid and octadecanoic acid are known for their ability to form hydrophobic films on metal surfaces, thereby reducing corrosion. The presence of phenolic derivatives contributes to corrosion inhibition through electron donation and antioxidant properties. Aromatic compounds, including benzene derivatives, enhance adsorption through π-electron interactions with the metal surface. Additionally, phytol and other long-chain compounds improve surface coverage, forming a protective barrier against the corrosive environment. The combined presence of these compounds enhances the inhibition efficiency of the extracts, leading to improved corrosion protection.

Meanwhile, The functional groups identified from FTIR analysis and the compounds detected through GC–MS analysis collectively explain the corrosion inhibition behavior observed in electrochemical studies. The adsorption of these phytochemicals onto the metal surface leads to the formation of a protective film, as evidenced by increased charge transfer resistance and reduced corrosion current density.
This confirms that the inhibition mechanism is governed by the interaction of organic molecules with the metal surface through both physisorption and chemisorption processes.

4. Conclusion

This study shows that rice husk and African breadfruit husk extracts act as effective green corrosion inhibitors for mild steel in a nitric acid medium. Both extracts significantly reduced corrosion rates, with African breadfruit husk extract exhibiting slightly higher inhibition efficiency under identical conditions. Electrochemical and surface analyses suggest mixed-type inhibition behaviour and adsorption-controlled protection mechanisms. The inhibitory performance is due to the combined effects of multiple phytochemical constituents present in the extracts rather than a single-component species. These findings highlight the potential of agro-waste-derived inhibitors for sustainable corrosion control in acidic environments; however, further studies involving detailed compound characterization and evaluation of alternative adsorption isotherms are required to better elucidate the inhibition mechanism

References

Abd El-Lateef, H. M., & Abo-Riya, M. A. (2013). Corrosion inhibition of carbon steel in acidic solution using a novel synthesized Schiff base: Electrochemical and surface morphology studies. Corrosion Science, 73, 171–182.

Abiola, O.K., Oforka, N.C. & Ebenso, E.E.(2007). Eco-friendly corrosion inhibitors: inhibitive action of Delonix regia extract for the corrosion of aluminum in acidic medium. Antoi-Corrosion Methods and Materials, 54,219 - 224.

Adeyemo, A.A., Olusegun, S.J., & Adekunle, A.S.(2021). Corrosion inhibition of mild steel in acidic medium by extracts of African breadfruit husk. Journal of Materials science and chemical engineering, 9(1),1-13.

Aisida, S.O., Mohammed, R., & Oyewo, O.O.(2021). Corrosion inhibition of mild steel in nitric acid solution by African breadfruit husk extract. Materials Today: Proceedings, 46,7522-7528.

Alaneme, K. K., Daramola, Y. S., Olusegun, S. J., & Afolabi, A. S. (2015). Corrosion inhibition and adsorption characteristics of rice husk extract on mild steel immersed in 1 M H_2SO_4 and HCl solutions. International Journal of Electrochemical Science, 10, 3553–3567.

Bai, M., Li, Y., Liu, X., & Hou, B. (2018). Synergistic effect of two plant extracts on the corrosion inhibition of mild steel in acidic media. Journal of Environmental Chemical Engineering, 6(4), 5364-5373.

Bentiss, F., Lebrini, M., & Lagrenée, M. (2005). Thermodynamic characterization of metal dissolution and inhibitor adsorption processes in mild steel/2,5-bis(n-thienyl)-1,3,4-thiadiazoles/hydrochloric acid system. Corrosion Science, 47(12), 2915–2931.

Boubakri, A., Dhouibi, L., & Derja, A.(2020). Green corrosion inhibitors, metals and alloys: A review. Journal of Environmental Chemical Engineering, 8 (4), 103946.

Bouklah, M., Hammouti, B., Lagrenée, M., & Bentiss, F. (2006). Thermodynamic properties of 2,5-bis(4-methoxyphenyl)-1,3,4-oxadiazole as a corrosion inhibitor for mild steel in normal sulfuric acid medium. Corrosion Science, 48(9), 2831–2842.

Ebenso, E.E., N.O. & Odiongenyi , A.O. (2008). Corrosion inhibitive properties and absorption behavior of Piper guinensis as a green corrosion inhibitor for mild steel in H2SO4 using 2,2-acetylpenolthiazine. Material Chemistry and Physics, 79(1), 58-69.

Eddy, N.O. & Mamza, P.A.P. (2009). "Inhibitive and adsorption properties of ethanolic extract of seeds and leaves of Azadirachta indica on the corrosion of mild steel in H_2SO4, Portugaliae Electrochima Acta, 27(4), 443-456.

Ehi-Eromosale, I.C., Adelabi, O.T., & Orodu, O.D (2020). Corrosion inhibition of mild steel in hydrochloric acid solution by African breadfruit husk extract. Journal of Environmental Chemical Engineering, 8(5), 104094.

Eddy, N. O., Ita, B. I., & Ibok, U. J. (2010). Adsorption, inhibitive properties, and thermodynamic characterization of green corrosion inhibitors for mild steel in acidic medium. Journal of Applied Electrochemistry, 40(2), 445–456.

Ibrahim, J., & Bishir, U. (2021). Corrosion inhibition potential of ethanol extract of Acacia nilotica leaves on mild steel in acidic medium

Khan, N., Khan, S.S., Pradhan, S.,& Quraishi, M.A.(2020). Corrosion inhibition performance of rice husk extract on mild steel in 1M HCl solution: Experimental and theoretical studies. Journal of molecular liquids, 302,112633.

Matori, K.A., Haslinawati, M.M.(2009)."Rice Husk as a substrate for Pure Silica Production." Journal of Materials Science and Technology, 25(6),653-658.

Mohammed, M. A., Abdullah, A.M., & Al-Mahdi, A.M (2021). Synergistic corrosion inhibition of mild steel in nitric acid solution by combined extracts of rice husk and African breadfruit husk. Journal of material science and chemical engineering,9(2), 1-14.

Moraes, M.A.,Jr.,V.E.Silva,J.A.S., Goncalves & J.L.F. Monteiro (2014). "Characterization of Rice Husk for use in combustion ."Journal of Materials Science and Engineering B, 4(1),1-9.

Nnanna, L.A., Uchendu , K.O., Nwosu , F.O., Ihekronye, U., & Eti , E.P. (2013). Gmelina arborea bark extracts as a corrosion inhibitor for mild steel in an acid environment. International Journal of Materials and Chemistry,4(2), 34-39.

Obi-Egbedi, N.O., I.B., & Umoren, S.A. (2021). Corrosion inhibition of mild steel in acidic medium by extracts of African breadfruit husk and rice husk: experimental, theoretical, and synergistic studies. Journal of molecular liquids, 322, 114711.

Okafor, P.C., Osabor, V. & Ebenso, E.E. (2007). Eco-friendly corrosion inhibitors: Inhibitive action of ethane extracts of Garcinia Kola for the corrosion of aluminum in acidic medium. Pigment Resin Technol. 36(5), 299-305.

Olawale, O. & Adediran, A.(2017)." Inhibitory Action of Rice Husk Extracts on Corrosion of Mild Steel in Acidic Medium."Journal of Materials Science and Chemical Engineering, 5(2), 14-25.

Singh,P.(2018). " Rice Husk Ash as a corrosion inhibitor for Mild Steel in Acidic Medium," Journal of Materials and Environmental Science, 9 (5), 1430-1438.

Umoren, S.A., Solomon, M.M., & Udobang, E.E.(2016). Inhibition of mild steel corrosion in acidic media by rice husk extract and African breadfruit husk extract. Journal of Adhesion Science and Technology, 30(12), 1345-1363.

Xu, B., Wang, W., Luo, J., & Ding, X. (2015). Synergistic effect of cinnamaldehyde and iodide ions on corrosion inhibition of mild steel in acidic media. Corrosion science, 103,201-210.